Edil, T. B. and Wang, X. (2000). "Shear Strength and K_0 of Peats and Organic Soils." *Geotechnics of high water content materials*, ASTM STP 1374, West Conshoho-cken, Pa., 209–225.

Hanrahan, E. T. and Rogers, M. G. (1981). "Road on peat: Observations and design." *J. Geotech. Eng. Div*., 107(10): 1403–1415.

Hobbs, N. B. (1986). "Mire Morphology and the Properties and Behavior of Some British and Foreign Peats." *Q. I Eng. Geol*., London, 19(1): 7-80.

Huat, B.B.K. (2004). "*Organic and Peat soil Engineering*." University Putra Malaysia, Serdang, Malaysia.

Janz, M. and Johansson S. (2002). "The Function of Different Binding Agents in Deep Stabilization," *Report 9, Swedish Deep Stabilization Research Center*, Linköping, Sweden.

Kalantari, B. and Huat, K. (2009). "Precast Stabilized Peat Columns to Reinforce Peat Soil Deposits." *The Electronic Journal of Geotechnical Engineering* (EJGE), Vol. 14, Bund. B.

Kazemian, S., Asadi, A. and Huat, B.B.K. (2009). "Laboratory Study on Geotechnical Characterization of Tropical Organic Soils and Peat." *International Journal of Geotechnics and Environment*. January, issue 1.

Kazemian, S., Huat B. B. K., Jit Ming Yeong, and Vahed, G. (2008). "Laboratory Investigations on Shear Strength of Organic Soils and Peat Reinforced with Cement Columns," *Proc. of Int. Graduate Con. on Eng. and Sci. (IGCES) UTM*, Johor Bahru, Malaysia.

Kogure, K., Yomuguchi, H., Ohira, Y. and Ishioroshi, H. (1986). "Physical and Engineering Properties of Peat Ground." *Proceeding Advances in Peat land Engineering*. Ottawa, Canada, 95-100.

Landva, A. O., and Pheeney, P. E. (1980). "Peat Fabric and Structure." *Canadian Geotechnical Journal*, 17(3), 416–435.

Larsson, S. (2003). "Mixing Processes for Ground Improvement by Deep Mixing", *Doctoral thesis published in Royal Institute of Technology, Stockholm*, Sweden.

Magnan, J. P. (1980). "Classification Geotechnique Des Sols: 1- A Propos De La Classification LPC." *Bulletin de Liaison des Laboratories des Ponts et Chaussees*, Paris, 19-24.

Mesri, G. & Ajlouni, M. (2007). "Engineering Properties of Fibrous Peats." *Journal of Geotechnical and Geoenvironmental Engineering*, ASCE, U.S.A., Vol. 133, No. 7.

Mesri, G. (1973). "Coefficient of Secondary Compression." *J. Soil Mech. and Found. Div*., 99(1), 123–137.

Mesri, G., and Godlewski, P. M. (1979). "Closure to Time and stress compressibility interrelationship." *Journal Geotechnical Engineering Div*., 105 (1): 106–113.

Mesri, G., Stark, T. D., Ajlouni, M. A., and Chen, C. S. (1997). "Secondary compr-ession of peat with or without surcharging." *Journal Geotechnical Geoenvironmental Engineering*, 123 (5), 411–421.

Yulindasari (2006). "Compressibility Characteristics of Fibrous Peat Soil." *Master of Engineering Thesis*, Universiti Teknologi Malaysia.

Von Post, L. (1922). "Sveriges Geologiska Undersoknings Torvinventering Och Nagre av Dess Hittills Vunna Resultat, Sr. Mosskulturfor." *Tidskr* 1: 1-27.

Bearing Capacity of Rectangular Foundations near the Slopes with Nonassociated Flow Rules

N. Ganjian[1], F. Askari[2], and O. Farzaneh[3]

[1] PhD Candidate in Geotechnical Eng., Civil Engineering Department, College of Engineering, University of Tehran, P.O. Box: 11365-4563, Tehran, IRAN; FAX: +982144404928; Email: nganjian@ut.ac.ir, Corresponding author.
[2] Assistant professor, International Institute of Earthquake Engineering and Seismology, Tehran, IRAN; Email: Askari@iiees.ac.ir
[3] Assistant professor, Civil Engineering Department, College of Engineering, University of Tehran; Email: ofarzane@ut.ac.ir

ABSTRACT

A method of three-dimensional slope stability analysis is presented here based on the energy consideration to obtain the ultimate bearing capacity of rectangular foundations located near the slopes with coaxial nonassociated flow rule. Taking the eccentrically loaded foundation into account, a rotational failure mechanism consisted of several lateral surfaces is considered. The stress distribution along the rupture surface, needed to obtain the rate of dissipation of internal energy for the nonassociated flow rule, is established on the basis of extended Bishop's method and boussinesq theorem. The bearing capacity of rectangular foundations in different conditions is obtained using the proposed method and the effects of dilatancy angle are investigated. The results indicate that for the nonassociated flow rule materials, the bearing capacity of slopes reduces with decrease in the dilatancy angle. These influences increase in the case of mild slopes in frictional.

KEY WORDS

Rotational Failure Mechanism; 3D Bearing Capacity; Nonassociated flow rule.

INTRODUCTION

The assessment of the stability of slopes under surcharge loads or the determination of ultimate bearing capacity of foundations located near the slopes is a fundamental problem received wide attention across geotechnical communities because of its practical importance. Previous studies show that, in such a complex footing-on-slope system, the ultimate bearing capacity of the footing may be governed by either the local foundation failure or the global slope failure. The non-eccentric loading, make this problem more difficult in superstructures located on top of the slopes under wind or earthquake conditions.

Numerous two-dimensional methods have been developed for the evaluation of stability of loaded slopes. However, all slope failures are three-dimensional (3D) in nature, especially for slopes under local loading. So, 3D stability analyses should be performed in the most cases of slope stability problems.

In general, proposed methods can be classified to the following types: a) Limit equilibrium approach. b) Characteristic line method. c) Limit analysis approach.

- The 3D limit equilibrium methods of columns, which are analogous to the two-dimensional methods of slices, have been most commonly used by engineers over the past several decades (Anagnosti, 1969; Hovland, 1977; Chen and Chameau, 1982; Ugai, 1985 and Hungr, 1987).

- The characteristic line method is based on integrating the equations of plastic equilibrium and is more rigorous, but still takes no account of the flow rule and can only deal with a restricted set of boundary conditions.

- In order to reduce the influence of the assumptions made in limit equilibrium methods, the methods of limit analysis (upper and lower bounds) based on the rigid plasticity theory were developed. In upper-bound theorem of limit analysis, it can be proved that the dissipation is a function only of the velocities. This property is used to compute the dissipation along the discontinuities, with the geometry being optimized to yield the minimum dissipated power and the lowest collapse load.

Some 3D upper-bound solutions have been presented assuming translational or rotational collapse mechanisms. Giger and Krizek (1976) used the upper-bound theorem of limit analysis to study the stability of a vertical corner cut subjected to a concentrated surcharge load. Michalowski (1989) presented a rigorous 3D solution for slope stability problems based on a translational collapse mechanism consisted of several rigid blocks which can also be used to estimate the bearing capacity of rectangular foundations. Farzaneh and Askari (2003) improved the results of Michalowski using combination of several lateral surfaces for each block and extended his 3D analysis for nonhomogenous soils. Farzaneh et al. applied this 3D multi-rigid block mechanism for stability analysis of convex slopes in plan view under local loading. De Buhan and Garnier (1998) evaluated the upper bound bearing capacity of square foundations located near a slope examining both rotational and punching collapse mechanisms.

Taking the truly 3D geometry of the problem into account, here, a 3D rotational collapse mechanism consisted of a log-spiral bottom surface and combination of several lateral surfaces is considered to improve the solutions for bearing capacity of foundations under combined loading.

Since the most granular soils do not obey the associated flow rule, this assumption in the upper bound methods causes some overestimation of volumetric strain and consequently overestimation of limit loads. Davis (1968) pointed out that consideration of the angle of dilatancy could better predict the limit load and it always tends to the lower limit loads. Although considering the nonassociated flow rule violates the basic assumption of the upper bound theorem, applying the energy balance in an admissible velocity field, leads to the ability of studying the effect of dilatancy angle in slope stability analysis.

There are some researches about the influences of dilatancy angle on 2D stability of loaded slopes (Yin et al., 2001 and Yang et al., 2007). However, the studies about the influences of nonassociated flow rule on the 3D stability problems are very limited according to the literature. In the present article, by considering the energy balance at collapse, bearing capacity of rectangular foundations are computed using the proposed rotational collapse mechanism for soils with nonassociated flow rules. Since the rate of dissipation of internal energy for a nonassociated material depends on the value of normal stresses along the rotational rupture surface, the stress distribution is established using the extended Bishop's method and Boussinesq theorem.

THREE-DIMENSIONAL FAILURE MECHANISM

Proposed rotational collapse mechanism, as an extension of 2D rotational mechanism, consisted of a log-spiral cylindrical bottom surface and combination of several lateral surfaces (shown in the Fig.1 as AEFD and BCFE). The known equation of bottom surface in polar coordinates is:

$$R = R_0 \exp[(\theta - \theta_0)\tan\phi] \tag{1}$$

where R_0 and θ_0 are the cylindrical coordinates of the start point of collapse on the surface and ϕ (=ψ) is the internal angle of friction.

Lateral surfaces can be adapted fulfilling the normality condition of upper-bound theorem through an equation of the following form:

$$z = f(r,\theta) \tag{2}$$

where (r, θ, z) are the cylindrical coordinates of a typical point P located on lateral surface. Compatibility of strains for associated materials means that at point P, the velocity vector across the surface makes an angle equal to the internal angle of friction (ϕ) with the tangent of slip surface or an angle equal to $\pi/2-\phi$ with the normal to the surface (**N**). Considering this assumption, the following differential equation can be driven:

$$\tan^2\phi\left(1+\left(\frac{\partial f}{\partial r}\right)^2\right) = \left(\frac{1}{r}\frac{\partial f}{\partial \theta}\right)^2 \tag{3}$$

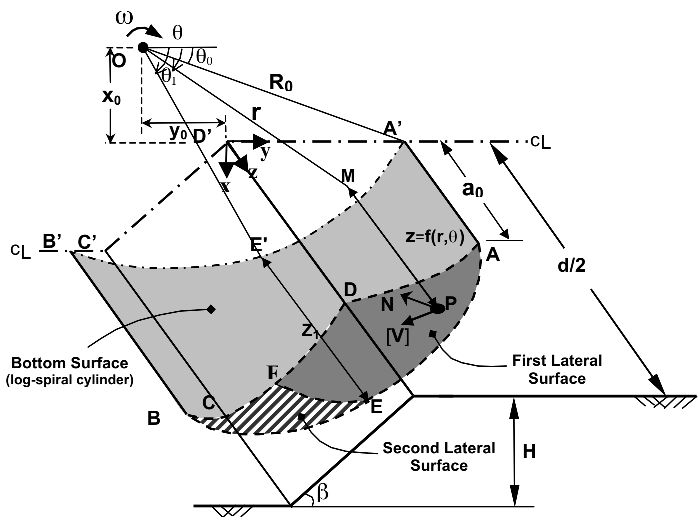

Figure 1. Proposed 3D collapse mechanism.

A possible class of solutions for above partial differential equation has been examined here as proposed by De Buhan and Garnier (1998):

$$z = f\ (r,\theta) = r \sinh(\theta \tan\phi + s) + b \tag{4}$$

where b and s are constants.

Considering a general point $A(R_0, \theta_0, a_0)$ on the lateral surface, the parameter b can be obtained as a function of parameters R_0 (which is itself a function of the coordinates of point O), θ_0, a_0 and s. Consequently, there are five independent geometrical variables (x_0, y_0, θ_0, a_0, and s) that should be optimized to obtain the critical failure mechanism.

De Buhan and Garnier (1998) used the rotational collapse mechanism with a lateral surface in each side to obtain bearing capacity of square foundations near the slopes. Performed analyses indicate that their proposed collapse mechanism extends laterally in frictional soils which results in overestimated limit loads.

To improve the results, combination of several lateral surfaces with the same rotational velocity and center of rotation, but different constant parameters (b_i and s_i), is proposed. For each additional lateral surface, two independent variables will be added to the five previous ones. Considering an arbitrary angle θ_1, coordinates of a point like E on the intersection of the bottom and first lateral surfaces, i.e. (R_1, θ_1, z_1), can be obtained. Crossing the second lateral surface from point E ($z_1 = R_1 \sinh(\theta_1 \tan\phi + s_2) + b_2$), b_2 is found as a function of θ_1 and s_2. In other words, the independent added variables are θ_1 and s_2. Based on the current study, a combination of three lateral surfaces in each side (with nine independent variables) is sufficient to obtain the appropriate results (Fig.2).

Many approaches have been developed to search for the critical failure mechanism in stability problems. Most procedures rely on traditional random generation techniques. The main limitation of these techniques is the uncertainty of the algorithm to find the global minimum limit load rather than the local minimum especially when the number of variable increases. Here, an alternative optimization method for determining the critical slip surface, called genetic algorithm (GAs), has been applied.

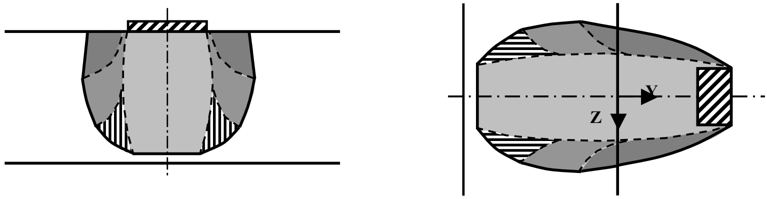

Front view **Plan view**

Figure 2. Schematic plans and front views of 3D rotational collapse mechanisms with combination of three lateral surfaces.

WORK AND ENERGY CALCULATIONS

Eq. 5 expresses the energy balance equation for a rigid collapse mechanism:

$$\int_A t_i [v]_i \, dA = \int_S T_i v_i \, dS + \int_V \gamma_i v_i \, dV \qquad (5)$$

where the left term represents the rate of work dissipated by the traction t_i over the velocity jumps ($[v]_i$ is the relative velocity between two adjacent rigid blocks), and the last two terms represent the rate of external work of traction T_i over velocities v_i at boundary S, and of body forces γ_i over velocities v_i in volume V.

Assuming the associated flow rule (normality condition) for a Mohr-coulomb material means that the velocity jump becomes normal to the yield line and inclined to the velocity discontinuity at friction angle ϕ, as shown in Fig.3(a). Therefore, for the linear Mohr-Coulomb yield function, the internal energy dissipation is:

$$t_i [v]_i = c[v]\cos\phi \qquad (6)$$

where, [v] is the resultant velocity jump and c is the cohesion of the material.

Thus, the internal energy dissipation will be independent of stresses along the rupture surfaces for associated materials.

In granular soils ($\psi \neq \phi$), assuming the normality condition, which is one of the main assumptions in the limit analysis theorem, generally causes the overestimation of volumetric strain. The effect of dilatancy angle on the stability of slopes can be investigated using a kinematically admissible velocity field comply with the kinematical boundary conditions and balancing the rate of internal energy dissipation with the rate of work of external forces.

As shown in Fig.3(b) for a nonassociated coaxial flow, the direction of [v] makes an angle ψ (dilatancy angle) with the plane of shear. The normal and shear stresses on the rupture plane representing E lie on a fictitious yield line, instead of the Mohr-Coulomb yield line. For this fictitious yield line we have:

$$\sigma_t = c^* + \sigma_n \tan\phi^* \tag{7}$$

where the values of the c^* and ϕ^* can be related by the following expressions (Davis, 1968):

$$\tan\phi^* = \eta \tan\phi \tag{8}$$

$$c^* = \eta\; c \tag{9}$$

$$\eta = \frac{\cos\psi \cos\phi}{1 - \sin\psi \sin\phi} \tag{10}$$

However, since the direction of [v] at the rupture plane is not normal to the supposed yield line, the internal energy dissipation will be obtained as:

$$t_i[v]_i = [v]\cos\psi \; [c^* + \sigma_n(\tan\phi^* - \tan\psi)] \tag{11}$$

Hence, in general, the energy expression depends on the distribution of normal stresses along the rupture surface for materials with nonassociated flow rule.

Drescher and Detournay (1993) proved that for translational collapse mechanisms, the limit load does not depend on the orientation of the velocity jump. So, a fictitious orientation and thus a fictitious flow rule (so as $\psi = \phi^*$) can be selected for which the specific energy dissipation is independent of σ_n:

$$t_i[v]_i = c^*[v]\cos\phi^* \tag{12}$$

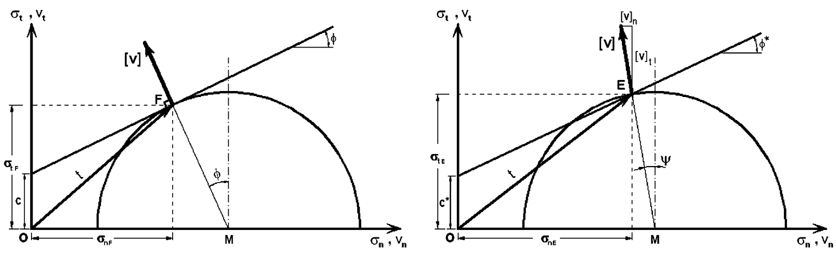

(a) (b)

Figure 3. Tractions and the direction of the velocity jump on the rupture plane for materials with (a) associated and (b) nonassociated flow rule.

However, in the case of rotational collapse mechanism, true orientation of the velocity jump should be considered. Thus, determination of the stress distribution along the rupture surface is necessary according to the Eq. 11.

Normal stress distribution along the rupture surfaces can be estimated using the limit equilibrium methods. Among the proposed methods of slices, Bishop's simplified method (Bishop, 1955) has been shown to produce somehow more accurate results when compared with other techniques. Hungr (1987) extended Bishop's method into three dimensions without any additional assumptions which expected to exhibit as a good performance as the original method. Here, the distribution of normal stresses along the proposed slip surfaces is generated by extension of Bishop's method considering fictitious yield line. More details and formulation of the extended Bishop's method into three dimensions is discussed by Hungr (1987). This limit equilibrium method of columns does not consider the shear resistance along the vertical sides of the sliding mass (Stark and Eid, 1998). In other words, the normal stresses generated by the earth pressure on the sides of the vertical columns along the vertical lateral surfaces are ignored. This will lead to an underestimation of the 3D factor of safety. Since the proposed lateral surfaces of used rotational collapse mechanism can be degenerated into vertical planes in the case of a nonassociated soil with ψ =0, removing mentioned limitation is imperative.

To include the normal stresses on vertical sides, at-rest earth pressure acting on the lateral vertical surface of the slide mass is considered as:

$$\sigma_n = k_0 \, \overline{\sigma}_v \tag{13}$$

where $\overline{\sigma}_v$ is the average vertical stress over the depth and k_0 is coefficient of earth pressure at rest (k_0 =1-Sin ϕ_d). The excess stresses on lateral surfaces due to surcharge load are also considered using the Boussinesq theorem.

COMPARISONS AND NUMERICAL RESULTS

Wei et al. (2009) studied about the 3D stability and failure mode of locally loaded slopes based on the strength reduction method (SRM) using numerical finite difference code (Flac3D). Here, to compare the current results with those of numerical methods, a locally loaded slope is considered. The slope geometry, dimensions of rectangular area of vertical loading and the soil properties are shown in Fig.4. Results of the analyses are compared in Table 1, for a loading q of 100 kPa and where the ratio of the loading length L to loading width B varies from 0 to 10.

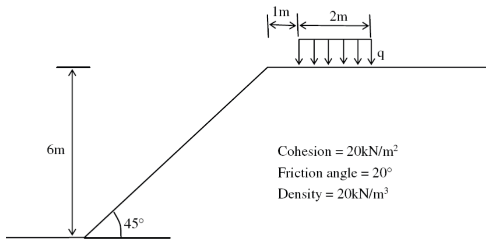

Figure 4. The geometry of the slope under local loading.

Table 1. Comparisons of safety factors for locally loaded slopes (q=100kPa)

L/B	**0**	**1**	**2**	**4**	**6**	**8**	**10**
WEI et al.	1.82	1.71	1.60	1.41	1.33	1.30	1.26
Farzaneh & Askari	1.94	1.82	1.63	1.43	1.35	1.29	1.26
Current	1.89	1.76	1.58	1.39	1.31	1.27	1.24

In the 3D analyses, when the loading ratio (L/B) is 1, 2, 4 and 6, the length of model chosen is 20m and when the L\B is 8 or 10, the length of model chosen is 30m. The results are nearly same as shown in this table, though the current results are somewhat less (better) for the slopes under rectangular foundations.

The described algorithm has been used to investigate the effects of nonassociativeness, or dilatancy angle, on the bearing capacity of rectangular foundations located near the slopes. Here, these effects are presented as some typical results.

Fig. 5 shows the influences of dilatancy angle (ψ) on the bearing capacity factor N'_c of a square foundation located in different distance from the slope (a/B) with the height of 6 meter and internal friction angle of ϕ=15° in the cases of centrically and eccentrically loading condition. Fig. 5(a) presents the bearing capacity factors versus